Human Molecular Genetics, 2020, Vol. 29, No. 14 2379–2394

doi: 10.1093/hmg/ddaa119
Advance Access Publication Date: 26 June 2020
General Article

GENERAL ARTICLE

Accelerated loss of hypoxia response in zebrafish with familial Alzheimer's disease-like mutation of presenilin 1

Morgan Newman[1,*], Hani Moussavi Nik[1], Greg T. Sutherland[2], Nhi Hin[1,3], Woojin S. Kim[4,5], Glenda M. Halliday[4,5], Suman Jayadev[6], Carole Smith[6], Angela S. Laird[7], Caitlin W. Lucas[7], Thaksaon Kittipassorn[1,8], Dan J. Peet[1] and Michael Lardelli[1]

[1]School of Biological Sciences, University of Adelaide, Adelaide, South Australia 5005, Australia, [2]Discipline of Pathology, School of Medical Sciences and Charles Perkins Centre, Faculty of Medicine and Health, The University of Sydney, Camperdown, New South Wales 2006, Australia, [3]Bioinformatics Hub, University of Adelaide, Adelaide, South Australia, Australia, [4]Brain and Mind Centre, Central Clinical School, Faculty of Medicine and Health, The University of Sydney, Camperdown, New South Wales 2052, Australia, [5]School of Medical Sciences, University of New South Wales and Neuroscience Research Australia, Randwick, New South Wales, Australia, [6]Department of Neurology, University of Washington, Seattle, Washington 98195, USA, [7]Centre for MND Research, Department of Biomedical Sciences, Faculty of Medicine and Health Sciences, Macquarie University, New South Wales 2109, Australia and [8]Department of Physiology, Faculty of Medicine Siriraj Hospital, Mahidol University, Bangkok 10700, Thailand

[*]To whom correspondence should be addressed at: 1.24 MLS Building, North Tce Campus, University of Adelaide, University of Adelaide, Adelaide, South Australia, Australia. Tel: +61 883134863; E-mail: morgan.newman@adelaide.edu.au

Abstract

Ageing is the major risk factor for Alzheimer's disease (AD), a condition involving brain hypoxia. The majority of early-onset familial AD (EOfAD) cases involve dominant mutations in the gene *PSEN1*. *PSEN1* null mutations do not cause EOfAD. We exploited putative hypomorphic and EOfAD-like mutations in the zebrafish *psen1* gene to explore the effects of age and genotype on brain responses to acute hypoxia. Both mutations accelerate age-dependent changes in hypoxia-sensitive gene expression supporting that ageing is necessary, but insufficient, for AD occurrence. Curiously, the responses to acute hypoxia become inverted in extremely aged fish. This is associated with an apparent inability to upregulate glycolysis. Wild-type *PSEN1* allele expression is reduced in post-mortem brains of human EOfAD mutation carriers (and extremely aged fish), possibly contributing to EOfAD pathogenesis. We also observed that age-dependent loss of HIF1 stabilization under hypoxia is a phenomenon conserved across vertebrate classes.

Received: March 24, 2020. **Revised:** May 27, 2020. **Accepted:** June 11, 2020

Introduction

Alzheimer's disease (AD) is the most prevalent form of dementia. Decreased levels of soluble amyloid-beta (Aβ) peptides in cerebrospinal fluid (1) (presumably due to decreased clearance from the brain) are regarded as one of the earliest markers of both early-onset familial AD (EOfAD) and late-onset sporadic AD (LOsAD), preceding disease onset by 20–30 years (2,3), while vascular changes may occur even earlier (4). When AD clinical symptoms eventually become overt, neurodegeneration may be too advanced for effective therapeutic intervention. This may explain the failure of drugs designed to inhibit supposed Aβ-related pathological processes to halt cognitive decline (5,6).

There are numerous observations implicating brain hypoxia in AD. For example, cardiovascular risk factors strongly correlate with LOsAD (7,8). Other significant LOsAD risk factors include vascular brain injury and traumatic brain injury (9), while recent studies suggest that aerobic exercise can reduce AD risk (10,11). Reduced blood flow has been observed in AD brains (12,13) most likely causing impaired oxygenation. Hypoxia can induce the expression of EOfAD genes/proteins (14–17) to drive Aβ production and a serum biomarker associated with hypoxia can predict which people with mild cognitive impairment (MCI) will progress to AD and which will not (18). An important controller of cellular responses to hypoxia is the heterodimeric transcription factor hypoxia-inducible factor 1 (HIF1), which is comprised of HIF1α and HIF1β monomers. HIF1α protein is decreased in LOsAD brains compared to age-matched controls (19), although the reason for this is unknown.

The molecular events underlying LOsAD are complex and have eluded detailed understanding. However, EOfAD is caused by inherited, dominant mutations in the genes, *presenilin 1* (*PSEN1*), *presenilin 2* (*PSEN2*), *amyloid beta A4 precursor protein* (*APP*) and *sortilin related receptor* (*SORL1*) (20,21) and so is amenable to genetic analysis in animal models. Only 5.5% of AD is defined as EOfAD (22). Nevertheless, the similarity in clinical disease progression and brain pathology of EOfAD and LOsAD (23) supports the assumption that genetic analysis of EOfAD will contribute to understanding of both forms of the disease.

PSEN1 and PSEN2 are alternative catalytic components of the γ-secretase complexes that cleave APP to form Aβ. On a population basis, ~60% of all EOfAD mutations occur in *PSEN1* (24) and are viewed mostly as altering the cleavage of APP to yield changes in the relative abundance of different Aβ size forms. Nevertheless, the exact relationship between EOfAD mutations in the *presenilin* genes and *APP* is still a matter of debate (25,26).

Structural and functional brain imaging (Magnetic resonance imaging (MRI) and/or positron emission tomography (PET)) from individuals with EOfAD mutations has revealed changes as early as 9 years of age (27,28). Elevations in Aβ deposition and reduced glucose metabolism have also been observed in EOfAD brains years before symptom onset (29). Surprisingly, there has been little detailed molecular investigation of the young adult brains of any animal model closely mimicking the human EOf genetic state—i.e. heterozygous for an EOfAD-related mutation in a single, endogenous gene. Therefore, to model and explore early changes in the brain driving AD pathogenesis, we have edited the zebrafish genome to introduce EOfAD-related mutations into the endogenous, *PSEN1*-equivalent gene of zebrafish, *psen1*. We recently published transcriptomic analyses of two such mutations, *psen1*^{K97fs} and *psen1*$^{Q96\_K97del}$ (30,31).

An analysis of the *psen1*^{K97fs} mutation in young and aged brains revealed that this mutation accelerates elements of brain ageing (31). However, we now know that this frameshift mutation differs from its human archetype (*PSEN2*^{K115fs}) in failing to restore the open reading frame (ORF) of various frameshifting alternative transcripts (31,32). (*All* EOfAD alleles of *PSEN1* and *PSEN2* follow the 'reading frame preservation rule' by producing transcripts encoding altered protein sequences without premature termination codons) (25,33). *psen1*^{K97fs} most likely represents a protein-truncating, hypomorphic allele similar to the human *PSEN1*^{P242fs} allele that causes the skin disease familial hidradenitis suppurativa without EOfAD (34). In contrast, the more EOfAD-like *psen1*$^{Q96\_K97del}$ mutation precisely deletes two codons thus following the reading frame preservation rule. It resembles numerous human EOfAD mutations by altering the structure of the first lumenal loop of PSEN1 (a multipass transmembrane protein of the endoplasmic reticulum and other organelles) (35).

A gene ontology analysis of young adult zebrafish brain transcriptomes revealed that, in contrast to *psen1*^{K97fs}, the more EOfAD-like *psen1*$^{Q96\_K97del}$ mutation is predicted to have very significant effects on mitochondrial function, especially synthesis of ATP, and on ATP-dependent functions such as the acidification of lysosomes that are critical for autophagy (36). The importance of oxygen for production of ATP by mitochondria, the apparent role of hypoxia in AD and the little-studied interaction between PSEN1 protein and HIF1α (37,38) led us to question whether our two zebrafish *psen1* mutants would differ in their responses to hypoxia with age.

We found that zebrafish brain gene expression responses to hypoxia increase greatly with age but that extremely aged brains 'invert' to show opposite responses. The hypomorphic and the EOfAD-like mutations of *psen1* both accelerate the onset of this inversion. Expression of the *psen1* gene itself under normoxia also increases with age until this reverses in extremely aged brains. Loss of *PSEN1* expression is also observed in human EOfAD brain tissue compared to age-matched controls supporting that these brains are subject to accelerated ageing. The more EOfAD-like mutation of *psen1* causes an abnormal, and possibly pathogenic, stabilization of a zebrafish HIF1α paralogue that becomes evident in aged brains.

Results

The ability to generate large families of siblings (over 100 individuals) and hold them in the same environment (the same tank) reduces genetic and environmental noise in omics analyses while allowing sampling of large numbers of individuals for statistical power. We have previously exploited this in our studies of EOfAD-related mutation model brain transcriptomes (31,32). In these studies, we typically generate families in which half the siblings are heterozygous mutants (modelling the human carriers of dominant EOfAD mutations) and half the siblings are non-mutant (i.e. wild-type). Serendipitously, not all the individuals of these large families are required for the omics analyses, so that follow-up experiments can be performed on individuals of various ages from families generated at various times. To investigate the interaction between age and our mutations on responses to hypoxia, we sampled families extant in our zebrafish facility. As the individuals involved were those surplus to the needs of planned omics studies, it was not always possible to analyse equal numbers of females and males. However, a principal component analysis of transcriptome data has not revealed sex to be a major determinant of zebrafish brain molecular state (see Supplementary Material, Fig. S1).

We exposed zebrafish to acute hypoxia by placement in oxygen-depleted water (0.6 ± 0.2 mg/L O_2) for 3 h after which they were rapidly euthanized and their brains removed for analysis.

Accelerated loss of hypoxia responses in ageing mutant zebrafish brains

During hypoxia, cells promote survival by adjusting their energy metabolism. In part, this is controlled at the transcriptional level by changes in the expression of hypoxia response genes (HRGs) (39). These genes include *PDK1* encoding pyruvate dehydrogenase kinase 1 that phosphorylates pyruvate dehydrogenase to inhibit conversion of pyruvate to acetyl-CoA (40). In this way, pyruvate is directed away from the tricarboxylic acid cycle and oxidative phosphorylation and into ATP production via anaerobic glycolysis. Thus, *PDK1* acts as a form of 'rheostat' to set the relative rates of anaerobic glycolysis and oxidative phosphorylation. To determine the effects of age and our *psen1* alleles on genetic responses to hypoxia, we used digital quantitative PCR (dqPCR) to assess transcript levels from four HRGs: *cd44a*, *igfbp3*, *mmp2* (41) and *pdk1* (42) in the brains of zebrafish exposed to normoxia or acute hypoxia.

Unexpectedly, the responses of heterozygous zebrafish carrying either of our two *psen1* mutant alleles were essentially identical and very different to those of wild-type siblings (Fig. 1A and B; Tables 1 and 2; Supplementary Material, Data S1). Young, 6-month-old mutants show increased basal levels of HRG expression under normoxia suggestive of pre-existing hypoxic stress, although other explanations are possible such as alteration of iron homeostasis or alteration of basal γ-secretase levels (see the Discussion). Nevertheless, both wild-type and mutant young adult zebrafish were able to increase HRG expression under acute hypoxia. Aged, 24-month-old wild-type zebrafish showed increased basal HRG expression under normoxia, resembling HRG expression in the young mutant animals (Fig. 1A and B; Tables 1 and 2; Supplementary Material, Data S1). This is consistent with our previous observation that the $psen1^{K97fs}$ mutation accelerates brain ageing (31). Despite their increased level of HRG expression under normoxia, the 24-month-old wild-type brains could still respond further to hypoxia with an approximately 2-fold increase in HRG expression. Interestingly, their levels of HRG expression were then very similar to those of normoxic 24-month-old $psen1^{K97fs}$ and $psen1^{Q96\_K97del}$ mutant zebrafish brains (Fig. 1A and B; Tables 1 and 2; Supplementary Material, Data S1), again supporting that these mutant brains are under hypoxic stress.

The greatest surprise came when aged, 24-month-old brains heterozygous for either *psen1* mutation were subjected to acute hypoxia. Rather than further upregulating HRG expression, they either failed to do this or they even downregulated HRG expression (Fig. 1A and B, *P*-values in Tables 1 and 2; Supplementary Material, Data S1). This inversion of the expected hypoxia response was particularly noticeable for expression of *pdk1*, suggesting an inability to upregulate anaerobic glycolysis in aged EOfAD-related mutant zebrafish under hypoxia. Assays of lactate content (a marker of anaerobic glycolysis) in brains both from young (7 months) and aged (31 months) $psen1^{Q96\_K97del}$ fish under acute hypoxia were consistent with this predicted failure to upregulate anaerobic glycolysis (Fig. 2). However, in contrast to *pdk1* expression, there was no apparent upregulation of anaerobic glycolysis in young wild-type brains under acute hypoxia (an observation also reported for young mouse brains under chronic hypoxia) (43).

If fAD-like mutations accelerate brain ageing, do wild-type brains eventually show the same failure of HRG expression as they age? To test this, we examined $psen1^{Q96\_K97del}$ mutant and wild-type sibling brains under normoxia or acute hypoxia at 42 months of age (Fig. 1B). (Laboratory-reared zebrafish are reported to have a mean life span of ~42 months (44), and we were fortunate enough to have $psen1^{Q96\_K97del}$ mutants and wild-type siblings surviving to this extreme age, however, there were no $psen1^{K97fs}$ mutants and their wild-type siblings available at this age). The levels of HRG expression in brains of both $psen1^{Q96\_K97del}$ mutants and wild-type siblings are essentially the same under normoxia, and both show downregulation of HRG expression under acute hypoxia (Fig. 1B). This clearly supports that fAD-like mutations accelerate brain ageing and that an inability to upregulate HRG expression under acute hypoxia may be an inevitable consequence of ageing.

Does decreased function of wild-type psen1 accelerate brain ageing?

Since age is the greatest risk factor for AD, the idea that EOfAD mutations of *psen1* might accelerate brain ageing seemed a parsimonious explanation for their pathogenicity. Therefore, we were surprised that both the less and the more EOfAD-like mutations of *psen1* appear to accelerate ageing in terms of HRG responses. This suggests the possibility that the levels of wild-type *psen1* allele expression are critical to the acceleration of brain ageing rather than the presence of the mutations themselves. Unfortunately, despite repeated attempts, so far we have been unable to generate an antibody with which to assay zebrafish Psen1 protein levels. However, dqPCR allows us to assay and compare the relative levels of wild-type and mutant *psen1* transcripts in zebrafish brains.

Premature termination codons commonly cause decreased mRNA transcript stability though the process of nonsense-mediated decay (NMD) (45). The $psen1^{K97fs}$ allele results in a premature termination codon (after 11 frameshifted amino acid codons) in exon 4 and its expression level is significantly decreased compared to transcripts from the wild-type *psen1* allele (Fig. 3A). This supports that the effects of $psen1^{K97fs}$ are due to loss of function. Indeed the expression level of the wild-type allele in the $psen1^{K97fs}$ heterozygous fish brains is approximately half that of wild-type sibling fish brains at both 6 months and 24 months of age (Fig. 3A). There is no evidence of upregulation of the wild-type allele in the $psen1^{K97fs}$ heterozygous fish such as might be caused by the phenomenon of 'genetic compensation' that can be driven by NMD (46). Note however that, if the $psen1^{K97fs}$ allele produces a truncated protein product, it is not expected to be completely without function (see Discussion).

The mutant transcripts in the EOfAD-like $psen1^{Q96\_K97del}$ heterozygous fish brains possibly show somewhat decreased expression compared to wild-type transcripts although this was not statistically significant (at the $P < 0.05$ level, Fig. 3B). However, unlike in the $psen1^{K97fs}$ heterozygous fish, the level of wild-type allele expression in heterozygous $psen1^{Q96\_K97del}$ fish brains is similar to that seen in wild-type siblings of the same age. Something must drive this increased level of wild-type allele expression. If the accelerated ageing of these fish is due to decreased wild-type allele function, then this could be due to interference from the mutant protein product of the $psen1^{Q96\_K97del}$ allele (see Discussion).

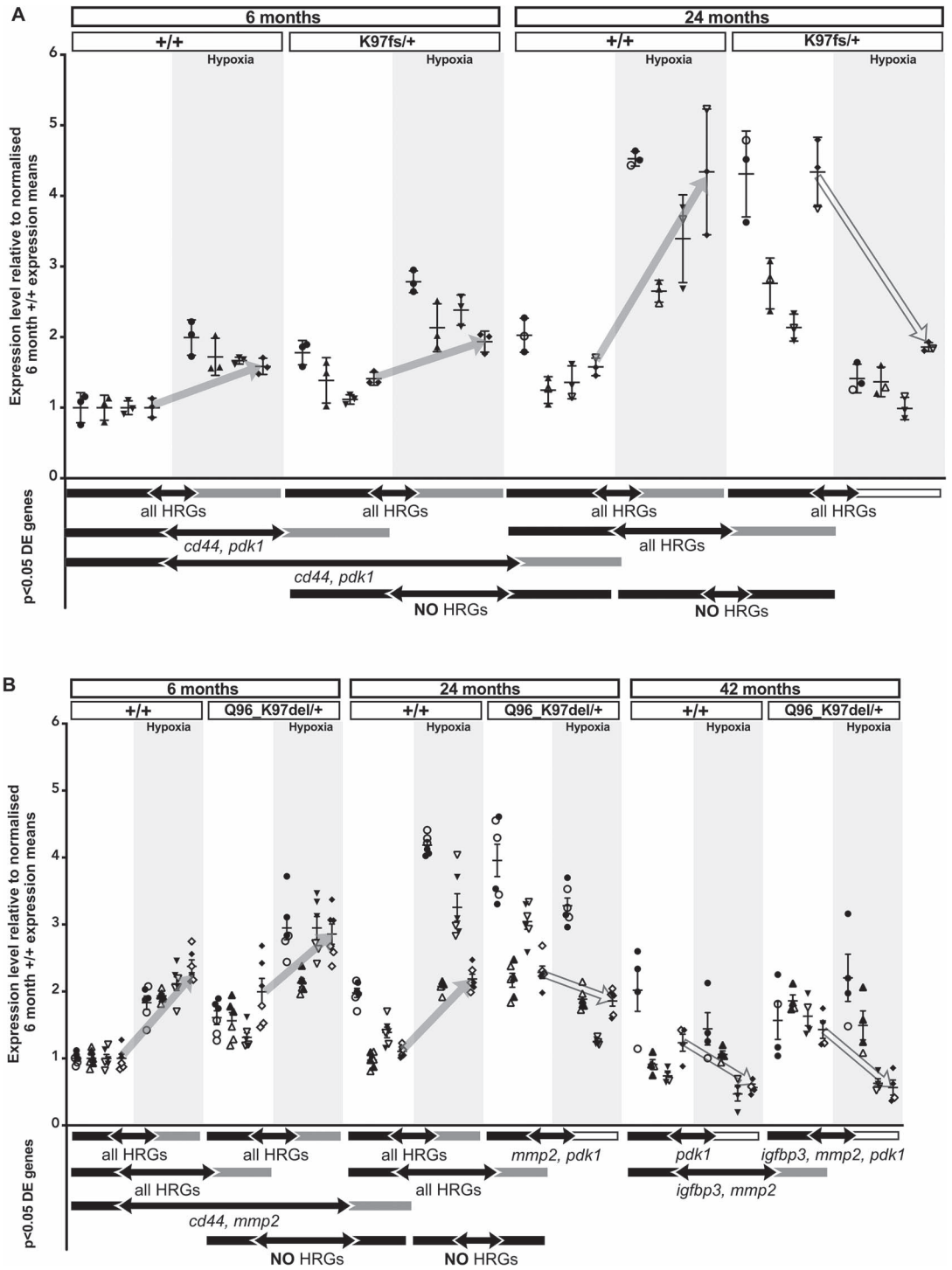

Figure 1. HRG expression in zebrafish brains under normoxia and hypoxia. Each data point on the graph indicates the relative transcript level for *cd44* (●), *igfbp3* (▲), *mmp2* (▼) and *pdk1* (♦) in 50 ng of cDNA generated from a single zebrafish brain RNA sample, assuming reverse transcription is complete (filled symbols, females; outlined symbols, males). Copy numbers for each transcript in each sample were scaled to the normalized means of the transcript copy numbers in the wild-type 6 months normoxia samples. The age and genotype of each sample are indicated at the top of the graph. Grey backgrounds indicate the hypoxia-treated samples. Wild-type (+/+), $psen1^{K97fs/+}$ (K97fs/+) heterozygous mutant and $psen1^{Q96\_K97del/+}$ (Q96_K97del/+) heterozygous mutant. *P*-value of < 0.05 for differentially expressed (DE) genes determined by *t*-test: two-sample assuming unequal variances. Solid lines flanking bidirectional arrows indicate comparisons in *t*-tests. The genes significantly DE are indicated below the bidirectional arrow. HRGs are HIF-1-responsive genes. The colour of the solid lines indicates the direction of differential expression; dark grey indicates increased expression and white (with dark grey outline) indicates decreased expression. Dark grey and white (with dark grey outline) arrows indicate the direction of pdk1 expression change under hypoxia (arrow ends connect pdk expression means). The raw dqPCR data, *P*-values and fold changes for all comparisons made are given in Tables 1 and 2 and Supplementary Material, Data S1. (**A**) HRG expression in K97fs/+ and +/+ siblings (6 months and 24 months). (**B**) HRG expression in Q96_K97del/+ and +/+ siblings (6 months, 24 months and 42 months).

Table 1. P-values calculated for comparisons of HRG expression in 6-month-old and 24-month-old zebrafish brains under normoxia and hypoxia (K97fs/+ versus +/+ siblings)

6 months	Normoxia, +/+ versus K97Gfs/+	+/+, Normoxia versus hypoxia	K97fs/+, Normoxia versus hypoxia	K97fs/+ normoxia versus +/+ hypoxia	
	$P =$	$P =$	$P =$	$P =$	
cd44a	0.00783228	0.006314391	0.001663059	0.28801924	
igfbp3	0.165463511	0.01694569	0.050922675	0.236891265	
mmp2	0.161245754	0.001817468	0.010295962	0.00032791	
pdk1	0.012157721	0.004652282	0.013814721	0.108391519	
24 months	Normoxia, +/+ versus K97Gfs/+	Hypoxia, +/+ versus K97Gfs/+	+/+, Normoxia versus hypoxia	K97fs/+, Normoxia versus hypoxia	K97fs/+ normoxia versus +/+ hypoxia
	$P =$	$P =$	$P =$	$P =$	$P =$
cd44a	0.00905243	0.000164359	0.000482095	0.015923746	0.606823905
igfbp3	0.00758629	0.000171843	0.000578267	0.010219623	0.660525701
mmp2	0.01134734	0.022886107	0.013072996	0.001327811	0.078629161
pdk1	0.011036627	0.040541648	0.033578682	0.013009494	0.997382256
6 months versus 24 months	Normoxia +/+, 6 months versus 24 months	Normoxia, K97fs/+ 6 months versus +/+ 24 months			
	$P =$	$P =$			
cd44a	0.005215672	0.221551983			
igfbp3	0.169616519	0.569035161			
mmp2	0.091145915	0.226718693			
pdk1	0.00559651	0.135261456			

Evidence for accelerated brain ageing in human EOfAD

Mutations of human *PSEN1* (or *PSEN2*) that prevent any ORFs from utilizing the original termination codon have never been seen to cause EOfAD (in line with the 'reading frame preservation rule') (25). A notable difference between the zebrafish $psen1^{K97fs}$ and $psen1^{Q96\_K97del}$ alleles is that only the latter obeys the reading frame preservation rule and only this EOfAD-like mutation upregulates wild-type *psen1* allele expression to equal or exceed that in wild-type fish. Does a similar upregulation of *PSEN1* gene expression occur in human EOfAD? To test this, we used dqPCR to examine wild-type and mutant *PSEN1* allele expression in three post-mortem EOfAD brains (medial temporal cortex region without significant neuropathology) and in healthy, age-matched controls (Fig. 4). Consistent with our $psen1^{Q96\_K97del}$ mutant data, transcripts of the mutant human mutant *PSEN1* allele were always detectable and at approximately half the level of the transcripts from the wild-type allele. However, expression of the wild-type allele was lower than in the age-matched controls (Fig. 4). We reasoned that, since mutation of *psen1* in zebrafish appears to accelerate brain ageing and since the human EOfAD brains were from people who had died from this disease, their decreased human *PSEN1* expression might represent a phenomenon more similar to gene expression in extremely aged fish brains. Therefore, we compared the relative *psen1* gene expression levels between the young (6 months), aged (24 months) and extreme aged (51 months) wild-type female fish brains. (Mutant fish brain cDNAs were not available for this experiment.) We observed the expected increase in *psen1* expression from 6 to 24 months but then a significant decrease in expression by 51 months (Fig. 5). This supports that human brains with overt EOfAD may display the equivalent of an 'extremely aged' molecular state giving them a lower level of *PSEN1* expression than chronologically age-matched healthy brains that are, in reality, less aged biologically.

Interestingly, the age-dependent changes in brain transcript expression of a zebrafish paralogue of *HIF1α* (*hif1ab*) mirror closely those of *psen1* expression but are very different from its protein expression (see below and Fig. 6).

Loss of HIF1 in aged brains is conserved across vertebrate species

HIF1α is one component of the heterodimeric transcription factor HIF1 that plays an important role in cellular responses to hypoxia. Hypoxia increases the stability of HIF1α protein, thus increasing HIF1 levels and upregulating a large number of HRGs. In a study of brain ageing and responses to hypobaric hypoxia in rats, Ndubuizu *et al.* (47,48) observed an inability to stabilize Hif1α under hypoxia after 18 months of age. To test whether this phenomenon might explain the inability of extremely aged zebrafish brains to upregulate HRGs in response to acute hypoxia, we used an antibody against the paralogous zebrafish protein Hif1ab. We observed that wild-type zebrafish already fail to stabilize Hif1ab from 24 months of age (Fig. 7A and B), at a time when their basal HRG expression is raised compared to younger fish, and during which they can still greatly increase HRG expression under hypoxia (as shown in Fig. 1). This shows that a failure to stabilize Hif1a in aged vertebrate brains is a characteristic conserved over an evolutionary period of greater than 430 million years (i.e. since the divergence of the teleost and tetrapod lineages) (49) but this does not explain the 'inversion' of HRG expression responses to hypoxia in aged zebrafish brains.

Table 2. P-values calculated for comparisons of HRG expression in 6-month-old and 24-month-old zebrafish brains under normoxia and hypoxia (Q96_K97del/+ and +/+ siblings)

6 months	Normoxia, +/+ versus Q96_K97del/+	+/+, Normoxia versus hypoxia	Q96_K97del/+, normoxia versus hypoxia	Q96_K97del/+ normoxia versus +/+ hypoxia	
	$P =$	$P =$	$P =$	$P =$	
cd44a	0.001345558	1.86483E-05	0.000179018	0.072598115	
igfbp3	0.003367147	2.27148E-09	0.00397462	0.02465246	
mmp2	0.005874266	1.3017E-05	4.79431E-05	0.000111507	
pdk1	0.003270849	8.95189E-07	0.007483553	0.130392718	
24 months	Normoxia, +/+ versus Q96_K97del/+	Hypoxia, +/+ versus K97Gfs/+	+/+, Normoxia versus hypoxia	Q96_K97del/+, normoxia versus hypoxia	Q96_K97del/+ normoxia versus +/+ hypoxia
	$P =$	$P =$	$P =$	$P =$	$P =$
cd44a	0.00083616	0.000107684	2.94348E-10	0.094123248	0.394019836
igfbp3	1.53017E-05	0.03464859	2.94718E-08	0.066237546	0.427249042
mmp2	8.07458E-07	0.000183921	5.86897E-05	1.97472E-05	0.386488096
pdk1	2.03058E-05	0.010855063	3.0078E-06	0.004855014	0.408870671
42 months	Normoxia, +/+ versus Q96_K97del/+	Hypoxia, +/+ versus Q96_K97del/+	+/+, Normoxia versus hypoxia	Q96_K97del/+, normoxia versus hypoxia	Q96_K97del/+ normoxia versus +/+ hypoxia
	$P =$	$P =$	$P =$	$P =$	$P =$
cd44a	0.328796317	0.134697144	0.197046713	0.209525094	0.747621218
igfbp3	0.000483699	0.066773494	0.411560109	0.008598631	0.000178563
mmp2	0.004127582	0.225910368	0.924628722	0.003053477	0.00414743
pdk1	0.322016804	0.994950955	0.008062354	0.002345495	0.003389143
6 months versus 24 months	Normoxia +/+, 6 months versus 24 months	Normoxia, Q96_K97del/+ 6 months versus +/+ 24 months			
	$P =$	$P =$			
cd44a	3.82053E-06	0.014740525			
igfbp3	0.701769718	0.002526586			
mmp2	0.00343619	0.493485411			
pdk1	0.189449494	0.007242434			

The EOfAD-like mutation of psen1 drives age-inappropriate stabilization of a HIF1 paralogue under acute hypoxia

Only one previous study, De Gasperi *et al.* (37), has noted that PSEN1 protein directly physically interacts with HIF1α. Using immortalized mouse embryonic fibroblasts these authors noted that Psen1 is required for stabilization of Hif1α under chemical mimicry of hypoxia using $CoCl_2$ or when treated with insulin. When mouse *Psen1* expression was replaced in these cells by human EOfAD mutant $PSEN1^{M146V}$, stabilization of Hif1α under chemical mimicry of hypoxia was normal but Hif1α stabilization due to insulin treatment was deficient. Our analysis of Hif1ab stabilization under acute hypoxia in aged, 24 month, zebrafish revealed a surprising difference between the heterozygous putative null mutant brains and EOfAD-like mutant brains. The EOfAD-like $psen1^{Q96\_K97del}$ brains stabilized Hif1ab under acute hypoxia, at an age when neither the wild-type or $psen1^{K97fs}$ brains did this (Fig. 7). The consequences of this age-inappropriate stabilization of Hif1ab are currently unknown but this observation emphasizes the importance of observing EOfAD-like mutation activities in aged, non-transgenic animal models.

Discussion

The production of energy supports all other cellular functions and is, therefore, fundamental to cellular, tissue, organ and organismal health. As the human brain ages, vascular function gradually declines (12,13) making it more difficult to deliver oxygen and energy substrates to support the brain's energy needs. As a consequence, transcription of *HIF1α* increases in the brain with age (50). Increased HIF1, acting to increase expression of *PDK1*, would be expected to raise the rate of anaerobic glycolysis to maintain production of ATP (that is necessary, among other things, for maintaining the solubility of proteins to prevent the protein aggregation characteristic of neurodegenerative conditions) (51). However, a primary diagnostic marker of AD brains is that they are hypometabolic with both reduced oxygen and glucose consumption (as revealed by brain imaging studies) (12,19). Also, Liu *et al.* (19) found evidence for reduced levels of HIF1α protein in post-mortem sporadic AD brains compared to normal, aged-matched controls. Recently, machine learning was employed to analyse structural MRI data from healthy controls and patients with dementia and other neurological conditions (52). This revealed distinct patterns of accelerated brain ageing

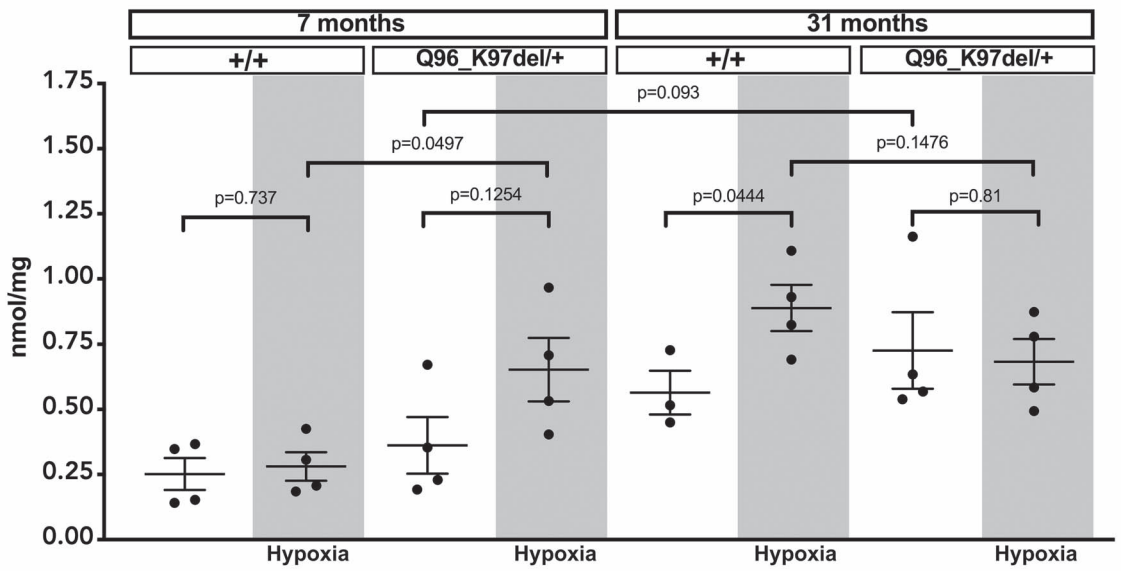

Figure 2. Lactate in 7-month-old and 31-month-old zebrafish brains under normoxia and hypoxia. Each data point on the graph indicates lactate content in a single whole zebrafish brain. All zebrafish were female. The age and genotype of each sample are indicated at the top of the graph. Grey backgrounds indicate the hypoxia-treated samples. Wild-type (+/+) and *psen1*$^{Q96\_K97del/+}$ (Q96_K97del/+) heterozygous mutant. *P*-values are calculated using *t*-test: two-sample assuming unequal variances. Raw lactate assay data is given in Supplementary Material, Data S2. Lactate concentration is expressed as nmol per mg of whole brain from Q96_K97del/+ zebrafish and their +/+ siblings.

in the dementia patients. These observations, together with our previous zebrafish *psen1* mutation data showing acceleration of ageing at the level of gene expression (31) and the hypoxia response data we have presented here, are consistent with a view of AD as both a consequence of ageing and as a pathological, hypometabolic brain state.

The clarity of the responses we have observed in whole zebrafish brains is due to our ability to place these entire, tiny ~7 mg brains under acute hypoxia. The human brain is ~250 000-fold larger in mass than a zebrafish brain, and the hypoxia it experiences as a result of failing vascular function would be expected to be regional (i.e. depending on the energy demand and vascularization of different brain regions) and would spread progressively as vascular function decreases (53,54). Notably, Raz *et al.* (55) recently observed that hypoxic hypoperfusion in rat brain drives hyperphosphorylation of tau while Mesulam (56) noted over two decades ago that the spread of neurofibrillary tangles of hyperphosphorylated tau in human brains tracks closely with the cognitive changes of AD progression (in contrast to Aβ plaque pathology). This is further evidence that hypoxia plays an important role in AD pathogenesis.

Our data from this study are also consistent with the 'stress threshold change-of-state' model of AD progression we presented previously (26). That model postulates aged brains 'inverting' (in terms of numerous molecular characteristics) into a pathological state as they reach a homeostatic threshold such as a limit in their ability to cope with the increasing oxidative stress caused by age-related hypoxia. A number of 'inversion' phenomena during AD pathogenesis have previously been noted by others. For example, in a transcriptome-based comparison of various brain regions in normal aged control, MCI and AD post-mortem individuals, Berchtold *et al.* (57) saw upregulation in MCI of genes involved in many cellular processes including mitochondrial energy generation. Many of these genes were subsequently downregulated in AD relative to controls. Similar observations have been made for the onset of dementia in Down syndrome individuals (58). Also, Arnemann *et al.* (59) also saw widespread elevation of metabolic brain network correlations during healthy ageing but reduction of such correlations in AD.

Digital, dqPCR facilitates comparison of the levels of different transcripts by allowing comparison of PCRs based on different primer pairs. Using dqPCR we could observe significantly decreased levels of *psen1*^{K97fs} transcripts compared to wild-type transcripts, presumably due to the mutant transcripts including a premature termination codon and so being subject to NMD. This supports a mainly hypomorphic phenotype for this allele. Any truncated protein product of *psen1*^{K97fs} in heterozygous brains would lack its own γ-secretase catalytic activity. However, it would likely resemble the truncated PSEN2 isoform PS2V (60,61) and so might enhance the γ-secretase activity provided by the wild-type allele, as well as inhibiting the cellular unfolded protein response (60,62). In contrast, transcripts of the *psen1*$^{Q96\_K97del}$ allele were not significantly less stable than wild-type transcripts in heterozygous brains, and their presence stimulated increased expression of the single wild-type allele. We speculate that this might be due to the mutant protein product of *psen1*$^{Q96\_K97del}$ interfering with the function of the wild-type Psen1 protein, either through interference with the formation of Psen1 holoprotein multimers (25), or through dominant inhibition of γ-secretase activity (63). If either of these actions caused increased oxidative stress (e.g. by interfering with mitochondrial function) (35,64), this might upregulate the expression of *psen1* (14). Notably, in wild-type fish, we observed an increase in *psen1* and *hif1ab* transcript levels with age that subsequently decreased as the fish became extremely aged, demonstrating once again the 'inversion' of gene expression with extreme age.

In post-mortem human carriers of three different *PSEN1* EOfAD mutations, we observed severely decreased *PSEN1* transcript expression in middle temporal gyrus tissue relative to healthy controls. If loss of *PSEN1* expression is also widespread in LOsAD brains, then this phenomenon may be important in AD

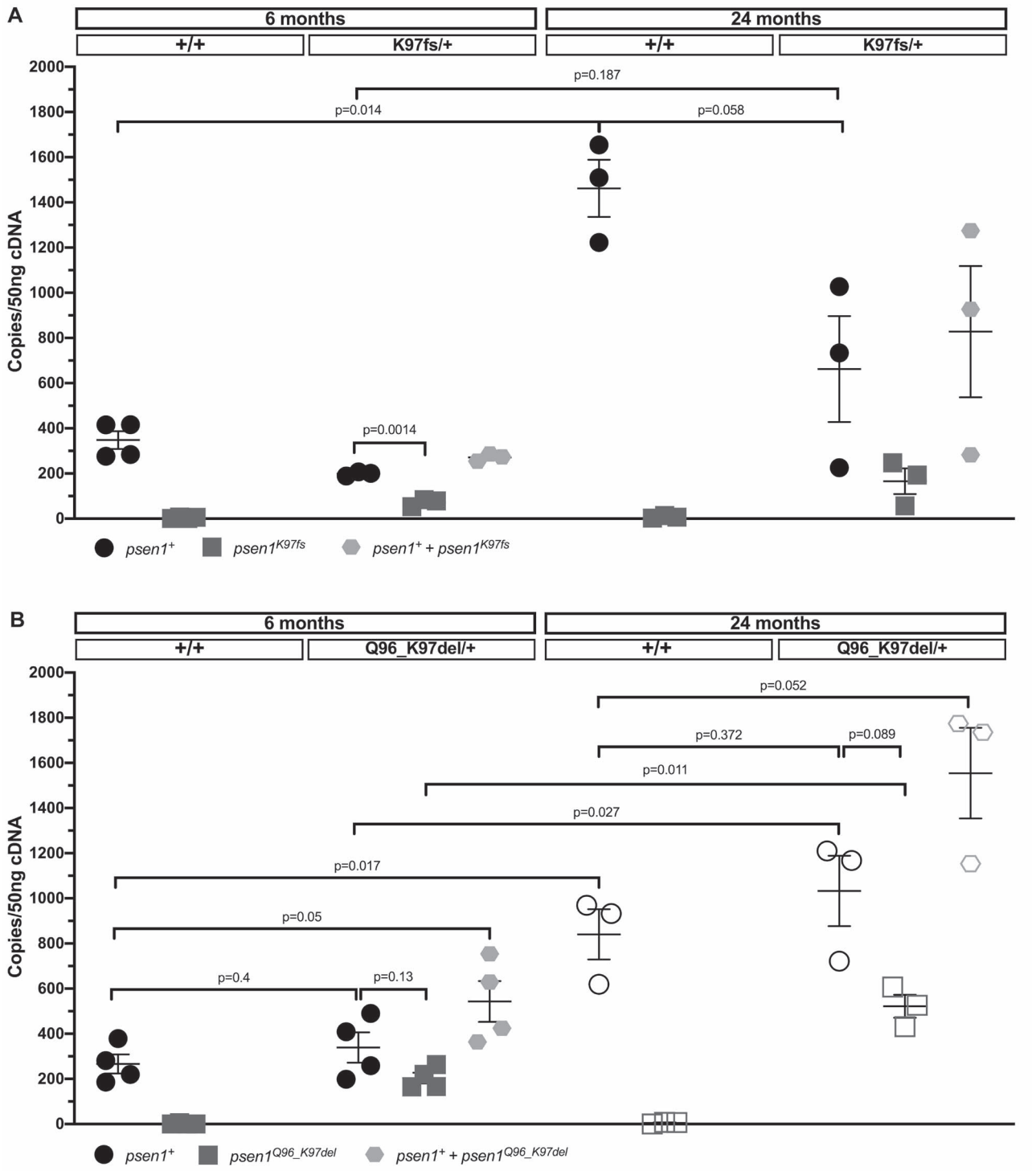

Figure 3. Allele-specific *psen1* transcript expression in 6-month-old and 24-month-old zebrafish brains. Each data point on the graph indicates *psen1* transcript copy number in 50 ng of cDNA generated from a single zebrafish brain RNA sample, assuming reverse transcription is complete. The age and genotype of each sample is indicated at the top of the graph. Wild-type (+/+), $psen1^{K97fs/+}$ (K97fs/+) heterozygous mutant and $psen1^{Q96\_K97del/+}$ (Q96_K97del/+) heterozygous mutant. *P*-values are calculated using *t*-test: two-sample assuming unequal variances. Raw dqPCR data and *P*-values are given in Supplementary Material, Data S4. (**A**) Allele-specific expression of either wild type psen1 (+, black circles) or mutant psen1 (K97fs, grey squares) or psen1+ and psen1K97fs combined (light grey hexagons) (all females). (**B**) Allele-specific expression of wild type psen1 (+, black circles) and mutant psen1 (Q96_K97del, grey squares) or psen1+ and psen1Q96_K97del combined (light grey hexagons) (filled symbols: females, outlined symbols: males). The 6-month-old and 24-month-old +/+ data are also included in Figure 5. They are included/repeated in this figure for comparison to data from their heterozygous mutant siblings.

pathogenesis. However, the published expression data for *PSEN1* in human LOs brain tissue show varying results depending on the brain region studied, the method of measurement, and which particular transcript variant was measured. For example, in LOsAD brains, a decrease in expression of *PSEN1* mRNA has been observed in the hippocampus (along with *PSEN2*) (65) and

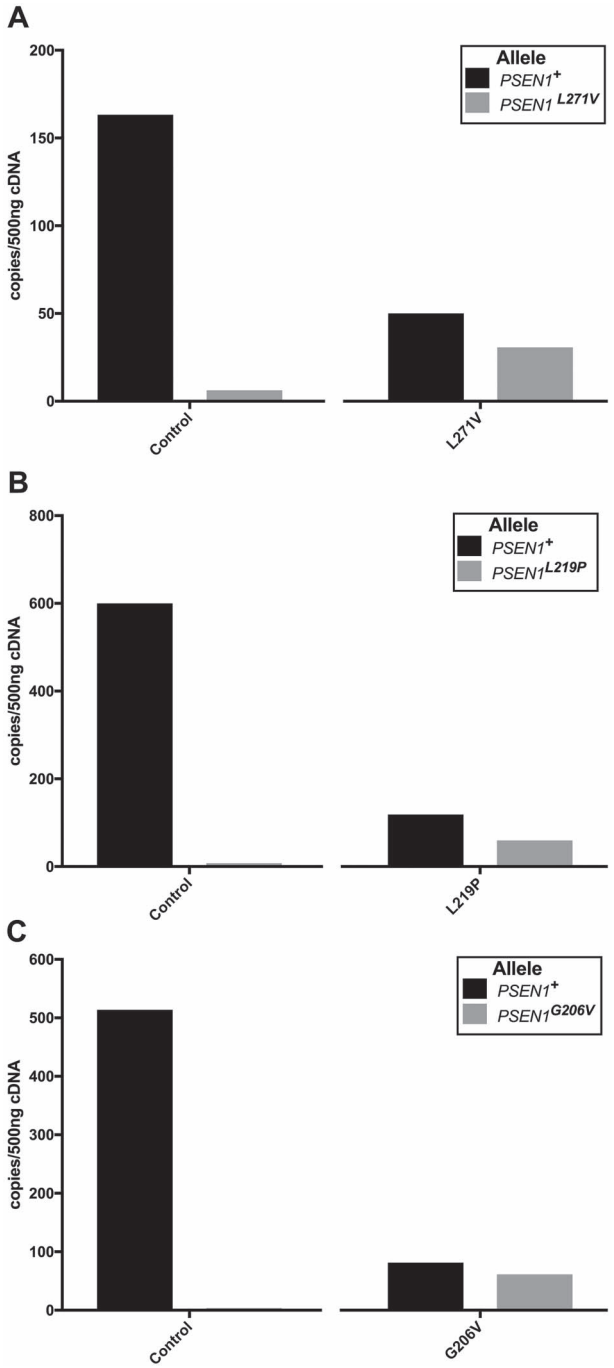

Figure 4. *PSEN1* transcript expression in the middle temporal gyrus region of brains of *PSEN1* mutation carriers and age-matched controls. Age-matched control (control, with corresponding mutation carrier sample in parentheses), $PSEN1^{L271V/+}$ heterozygous mutation carrier (L271V/+), $PSEN1^{L219P/+}$ heterozygous mutation carrier (L219P/+) and $PSEN1^{G206V/+}$ heterozygous mutation carrier (G206V/+). Raw dqPCR data is given in Supplementary Material, Data S3. (**A**) Expression of wild-type ($PSEN1^{+}$) and L271V mutant ($PSEN1^{L271V}$) alleles in control (51 years old) and L271V/+ (51 years old) cDNA samples. (**B**) Expression of either wild-type ($PSEN1^{+}$) and L219P mutant ($PSEN1^{L219P}$) alleles in control (60 years old) and L219P/+ (61 years old) cDNA samples. (**C**) Expression of either wild-type ($PSEN1^{+}$) and G206V ($PSEN1^{G206V}$) alleles in control (29 years old) and G206V/+ (32 years old) cDNA samples. The normalized *PSEN1* gene expression data (two different reference genes, *CYC1* and *RPL13*) is given in Supplementary Material, Data S3.

in the frontotemporal region (66) while an increase in expression of *PSEN1* mRNA has been measured in the temporal lobes (67,68) and superior frontal gyrus (68). Other studies reported no significant difference in *PSEN1* expression in LOsAD in the frontal cortex (69,70), the entorhinal cortex, the auditory cortex (although decreased *PSEN2* was observed) or the hippocampus (71). It is difficult to form any firm conclusions on *PSEN1* mRNA expression in LOsAD from these inconsistent findings. This should encourage more detailed analysis of *PSEN1* expression in both EOfAD and LOsAD brains in the future, particularly to compare the consistency of changes in mRNA level with changes in protein abundance.

While our observations are consistent with mutations in *PSEN* genes causing accelerated ageing, there are numerous studies that question the idea of AD being an inevitable consequence of age (72–74). Even if the failure to upregulate glycolysis under hypoxia we observed in extremely aged zebrafish is related to the brain hypometabolism of AD, this does not show that AD is an inevitable consequence of ageing. Rather, our results only support that age is a major risk factor for AD and may even be a necessary precondition for the disease.

Our study has uncovered a number of phenomena that we currently cannot explain. Why is it that, under acute hypoxia, 24-month-old zebrafish brains cannot stabilize Hif1ab but are still able to upregulate HRGs? Are there HIF1-independent systems activating HRGs such as PGC1α (a key regulator of cellular energy metabolism).(48)? Why does heterozygosity for only the EOfAD-like mutation in *psen1* (that does not truncate the open reading frame) allow unexpected stabilization of Hif1ab under hypoxia at an age when upregulation of HRGs fails? Indeed, why do transcript levels of HRGs decrease under hypoxia in these fish rather than increasing or, at least, not changing? Clearly, neither age nor the presence of mutations in *psen1* alone is sufficient to explain these phenomena and an interaction between the two factors is involved. One possible explanation would be that the *psen1* mutant brains are undergoing neurodegeneration. Indeed, our recent brain transcriptomic analyses on these two *psen1* mutations revealed alterations to inflammatory and immune pathways in aged *psen1* mutant brains (31,75). As inflammatory pathways are associated with neurodegeneration, these brains may be in the early stages of neurodegeneration or on a path towards it. However, a previous histological analysis of 24-month-old $psen1^{K97fs}$ heterozygous mutant brains did not find obvious pathology (31) and neither *psen1* mutation showed evidence of altered cell death pathways in transcriptomic analyses (31,75). Zebrafish have a high regenerative capacity following tissue damage that includes repair of nervous tissue (76) and previous attempts to model neurodegenerative diseases in adult zebrafish have failed to show cellular phenotypes (77). Therefore, we believe it unlikely that the effects we have seen in this study can be explained by the presence of significant neurodegeneration due to *psen1* mutation.

HIF1α has been shown to interact physically with PSEN1 protein (37,38) and a physical interaction of HIF1α with the γ-secretase complex (presumably via PSEN1) can increase γ-secretase activity (38). In turn, increased γ-secretase activity can increase HIF1α stability (and so HIF1 activity) via a p75NTR-dependent feed-forward mechanism (78). For this reason, and the known stabilization of HIF1α by ferrous iron deficiency (79,80) (that can be caused by failure of lysosomal acidification) (81), we are unable to assert with certainty that the increased basal HRG expression seen in our heterozygous *psen1* mutant brains is due to hypoxia. Further work will be required to dissect

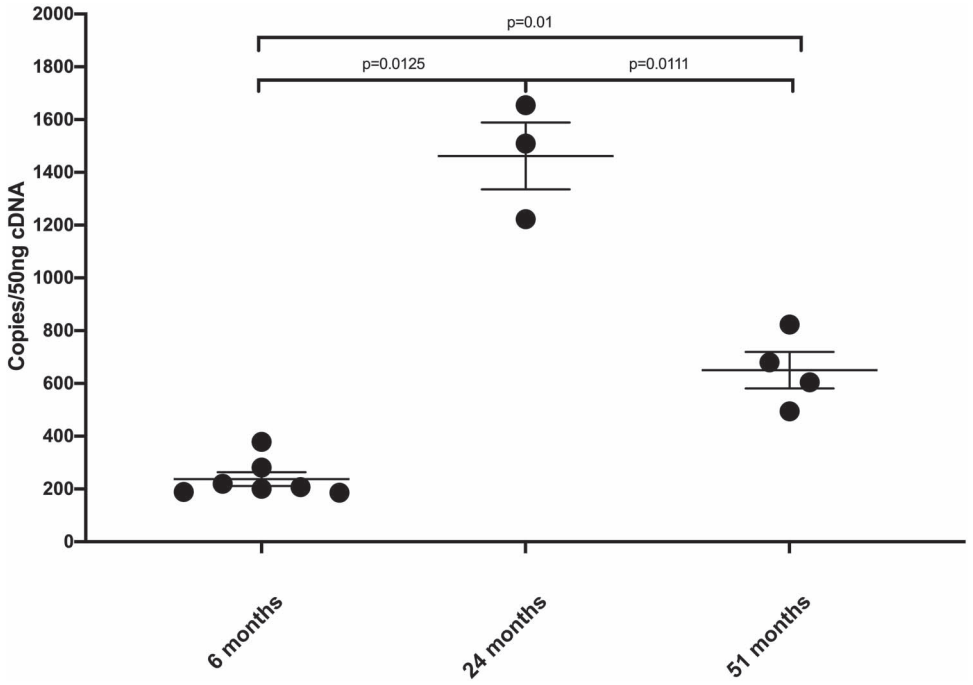

Figure 5. Wild-type *psen1* allele expression in 6-month-old, 24-month-old and 51-month-old wild-type zebrafish brains. Each data point on the graph indicates *psen1* transcript copy number in 50 ng of cDNA generated from a single zebrafish brain RNA sample, assuming reverse transcription is complete. All samples are wild-type females. The age of each sample is indicated at the bottom of the graph. *P*-values are calculated using *t*-test: two-sample assuming unequal variances. Raw dqPCR data are given in Supplementary Material, Data S3. Note that the data for the 6-month-old and 24-month-old samples are also presented in Figure 3. It is duplicated here for easy comparison to the 51-month-old samples.

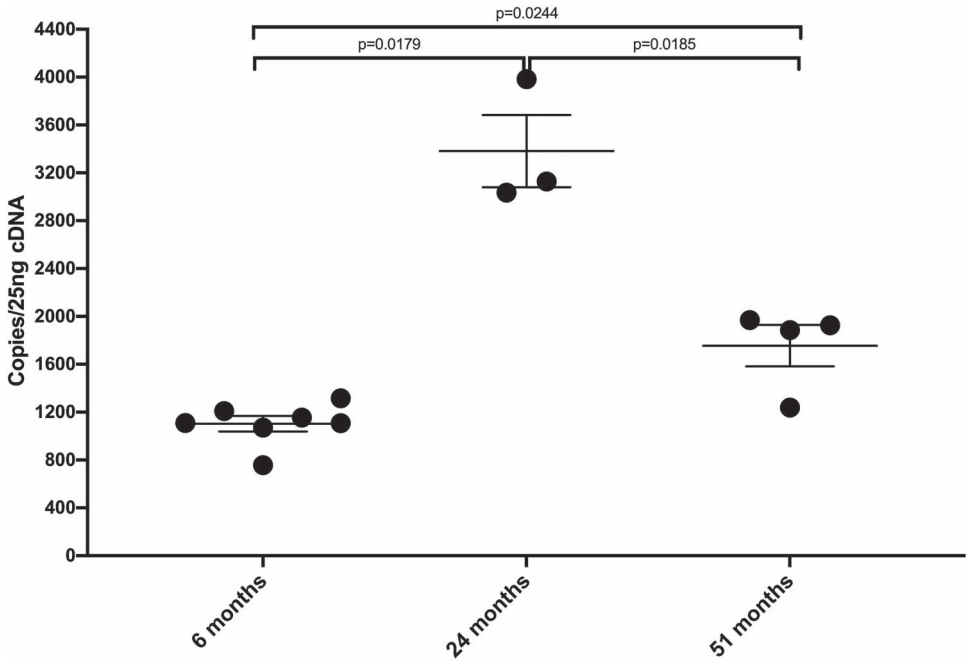

Figure 6. *Hif1ab* allele expression in 6-month-old, 24-month-old and 51-month-old wild-type zebrafish brains. Each data point on the graph indicates *psen1* transcript copy number in 25 ng of cDNA generated from a single zebrafish brain RNA sample, assuming reverse transcription is complete. All samples are wild-type female. The age of each sample is indicated at the bottom of the graph. *P*-values are calculated using *t*-test: two-sample assuming unequal variances. Raw dqPCR data are given in Supplementary Material, Data S4.

the influences of *psen1* mutations on HRG expression in young brains and to understand the inappropriate stabilization of Hif1ab in aged, EOfAD-like *psen1* mutant brains.

The experimental results described in this paper emphasize the intimate interaction between age, *PSEN1* (the majority locus for EOfAD mutations) and the HIF1 master controller of cellular hypoxia responses and energy metabolism. Maintaining vascular health and youthful brain hypoxia responses is likely a key to avoiding or delaying the onset of AD. For human EOfAD mutation carriers, a recent systematic review has revealed an association between physical exercise and better cognitive outcomes at expected symptom onset ages (82). This is

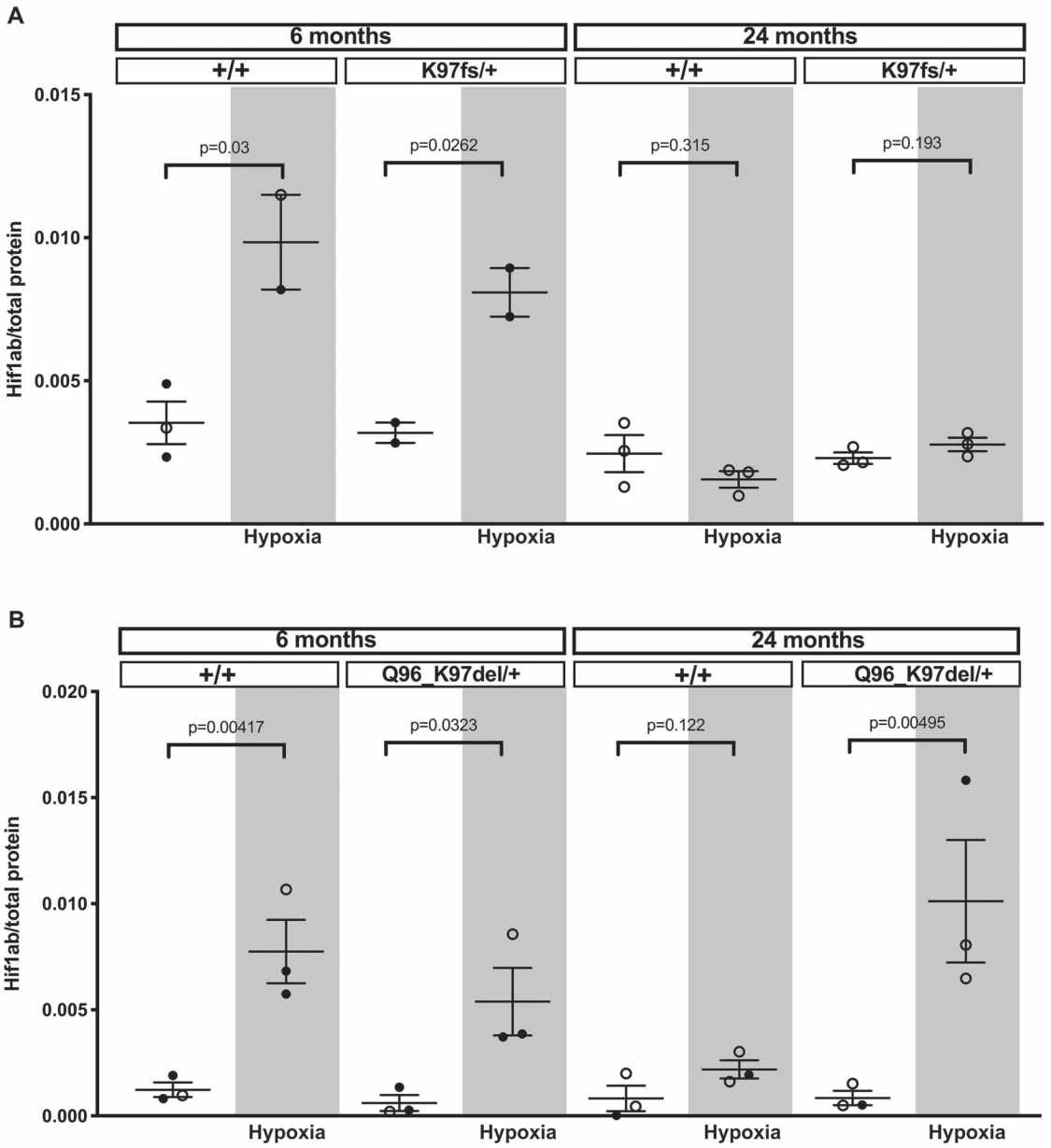

Figure 7. Hif1ab protein levels in 6-month-old and 24-month-old zebrafish brains under normoxia and hypoxia. Each data point on the graph indicates the Hif1ab protein level in protein extracted from a single zebrafish brain (filled circles, females; outlined circles, males). The age and genotype of each sample are indicated at the top of the graph. Grey backgrounds indicate the hypoxia-treated samples. Wild-type (+/+), *psen1*$^{K97fs/+}$ (K97fs/+) heterozygous mutant and *psen1*$^{Q96\_K97del/+}$ (Q96_K97del/+) heterozygous mutant. *P*-values are calculated using *t*-test: two-sample assuming unequal variances on Ln transformed data. Raw densitometry data and *P*-values are given in Supplementary Material, Data S5 and western blot images are shown in Supplementary Material, Figure S2. **(A)** Hif1ab protein level in K97fs/+ and +/+ siblings. **(B)** Hif1ab protein level in Q96_K97del/+ and +/+ siblings.

consistent with physical exercise being one of the few known protective treatments against LOsAD (83–86).

Materials and Methods

Zebrafish husbandry and animal ethics

All experiments, except for digital PCRs for *psen1* transcript expression in 6-month-old brains, were performed using Tubingen-strain zebrafish maintained in a recirculated water system. This work with zebrafish was conducted under the auspices of the Animal Ethics Committee of the University of Adelaide (permit no. 31945) and Institutional Biosafety Committee (IBC Dealing ID 122210). The digital PCRs for *psen1* transcript expression in 6-month-old brain experiments were performed using samples from Tubingen and AB-strain zebrafish maintained in a recirculated water system. This work with zebrafish was conducted under the auspices of the Macquarie University Animal Ethics Committee (permit no. 2015/034).

psen1 mutations

The isolation of the *psen1*^{K97fs} and *psen1*$^{Q96\_K97del}$ mutations has previously been described (31,30). Mutations were only analysed in the heterozygous state in this study.

Table 3. Human *PSEN1* mutations analysed for allele-specific dqPCR including age-matched control details. Post-mortem delay (PMD)

PSEN1 mutation	Codon change	Gender	Age at death (years)	Disease duration (years)	PMD (hours)	Project ID
L271V	CTG to GTG	Female	51	5	5	LA1
L219P	CTT to CCT	Female	61	7	13	LA2
G206V	GGT to GTT	Female	32	3	22	LA3
Control (L271V)	N/A	Female	51	N/A	41	LC2
Control (L219P)	N/A	Female	60	N/A	41	LC1
Control (G206V)	N/A	Female	29	N/A	40	LC3

Genomic DNA extraction and genotyping PCR of zebrafish tissue

DNA was extracted from adult zebrafish tail clips and genotyped via PCR as described in (31). Primers used for genotyping PCR were synthesized by Sigma-Aldrich Corp. St. Louis, Missouri, USA. Oligonucleotide sequences are given in Table 4.

Hypoxia treatment of adult zebrafish

Male or female adult zebrafish at the desired age and genotype were treated in low oxygen levels by placing zebrafish in oxygen-depleted water for 3 h (oxygen concentration of 6.6 ± 0.2 mg/L in normoxia and 0.6 ± 0.2 mg/L in hypoxia. Brains were subsequently used for digital PCR or western blotting analysis.

Whole brain removal from adult zebrafish

Adult fish were euthanized by sudden immersion in an ice water slurry for at least 30 s before immediate decapitation. The entire brain was then removed from the cranium for immediate RNA or protein extraction. All fish brains were sampled during late morning/noon to minimize effects of circadian rhythms. For the dqPCR *psen1* allele-specific experiments on 6-months-old zebrafish, whole heads were stored in RNAlater (Ambion, Inc, Foster City, California, USA, AM1312) prior to brain removal and total RNA extraction.

RNA extraction and cDNA synthesis of total adult zebrafish brain

Total RNA was extracted from whole zebrafish brain (~10 mg) using the (QIAGEN, Venlo, Netherlands, 74104) QIAGEN RNeasy Mini Kit according to the manufacture's protocol as described in (14,60). The RNA for dqPCR HRG experiments was DNase treated using RQ1 DNase from Promega (Madison, Wisconsin, USA) according to the manufacturer's instructions. The RNA for dqPCR *psen1* allele-specific experiments was DNase treated using the DNA-free™ Kit from Ambion, Life Technologies according to the manufacturer's instructions. RNA was quantified using a NanoDrop spectrophotometer. cDNA was synthesized using random hexamers and the Superscript III First Strand Synthesis System (Thermo Fisher Scientific, Waltham, Massachusetts, USA) according to the manufacturer's instructions.

RNA extraction and cDNA synthesis from human brain tissue

Human brain tissues were obtained from the Sydney Brain Bank at Neuroscience Research Australia and the NSW Brain Tissue Resource Centre at the University of Sydney. The brains were collected under institutional ethics approvals. Whole brains were sliced into blocks and fresh-frozen and stored at −80°C. Tissue samples from three cases with mutant *PSEN1* and three age- and gender-matched controls without significant neuropathology (see Table 3 for details) were processed for RNA extraction using TRIzol reagent (Invitrogen Camarillo, California, USA) following the manufacturer's protocol. All procedures were carried out using RNase-free reagents and consumables. Five micrograms of RNA were reverse transcribed into cDNA using Moloney-murine leukaemia virus reverse transcriptase and random primers (Promega) in a 20 µl reaction volume. RNA integrity was assessed with high resolution capillary electrophoresis (Agilent Technologies, Santa Clara, California, USA) and only RNA with RNA integrity number value greater than 6.0 was used.

3D Quant Studio Digital PCR

Digital PCR was performed on a QuantStudio™ 3D Digital PCR System (Life Technologies, Carlsbad, California, USA). Reaction mixes contained 1X QuantStudio™3D digital PCR Master Mix, Sybr® dye, 200 nM of specific primers and 12.5–500 ng cDNA (500 ng for *PSEN1* and *PSEN2*, 100 ng for *CYC1* and *RPL13*, 50 ng for *cd44a*, *igfbp3*, *psen1* 25 ng for *pdk1* and 12.5 ng for *mmp2*). The reaction mixture (14.5 µl) was loaded onto a QuantStudio™3D digital PCR 20 K chip using an automatic chip loader according to the manufacturer's instructions. Loaded chips underwent thermo-cycling on the Gene Amp 9700 thermo-cycling system under the following conditions: 96°C for 10 min, 39 cycles of 60°C (59°C for *CYC1* and *PSEN1G206V*site) for 2 min and 98°C for 30 s, followed by a final extension step at 60°C (or 59°C see above) for 2 min. The chips were imaged on a QuantStudio™ 3D instrument, which assesses raw data and calculates the estimated concentration of the nucleic acid sequence targeted by the Sybr® dye by Poisson distribution (87). Primers used were synthesized by Sigma-Aldrich and are listed in Table 2.

Protein extraction of total adult zebrafish brain

Each brain was homogenized in water supplemented with Sample Reducing Agent (10×, contains 500 mM dithiothreitol) (Thermo Fisher Scientific) and Complete Protease Inhibitors (Roche Life Sciences, Basel, Switzerland). LDS buffer (Thermo Fisher Scientific) was then added and the sample was briefly homogenized and placed at 90°C for 20 min. Each sample was divided into several aliquots. To generate a protein standard to allow quantitative comparison between signals on separate western blots, eight male non-mutant adult zebrafish at 6 months of age were selected and placed under hypoxia as described in (14). Protein was extracted from each brain as above. After extraction all homogenates were combined, thoroughly mixed and divided into several aliquots, with one aliquot being

Table 4. Primer sequences for genotyping, sequencing and dqPCR. WT denotes wild-type allele-specific PCR. The WT primer target site for *psen1* or *PSEN1* is indicated in parentheses

Gene symbol	Accession number	Target allele binding site	Sense primer (5′ → 3′)	Anti-sense primer (5′ → 3′)
Genotyping (genomic DNA)				
psen1	ENSDARG00000004870	*WT (K97 site)*	TCTGTCAGCTTCTACACACAGAAGG	CCATCCCTAAACTGCTCCTACTC
psen1	ENSDARG00000004870	*GAdel (K97fs)*	AATCTGTCAGCTTCTACACACAAGG	CCATCCCTAAACTGCTCCTACTC
psen1	ENSDARG00000004870	*CAGAAGdel (Q96_K97del)*	TGTCAGCTTCTACACAGACGGA	CCATCCCTAAACTGCTCCTACTC
psen1	ENSDARG00000004870	*WT (exon 4-intron)*	GGCACACAAGCAGCACCG	TCCTTTCCTGTCATTCAGACCTGCGA
psen1	ENSDARG00000004870	*WT-sequencing*	AGCCGTAATGAGGTGGAGC	N/A
dqPCR (cDNA)				
psen1	NM_131024	*WT (K97 site)*	CTACACACAGAAGGACGGACAGC	GCCAGGCTTGAATCACCTTGTA
psen1	NM_131024	*GAdel (K97fs)*	TCTGTCAGCTTCTACACACAAGGA	GCCAGGCTTGAATCACCTTGTA
psen1	NM_131024	*CAGAAGdel (Q96_K97del)*	TGTCAGCTTCTACACAGACGGA	GCCAGGCTTGAATCACCTTGTA
PSEN1	NM_000021.3	*WT (L271 site)*	CATTACTGTTGCACTCCTGATC	CTCCTGAGCTGTTTCAACCAG
PSEN1	NM_000021.3	*L271V mutation*	CATTACTGTTGCACTCCTGATC	CTCCTGAGCTGTTTCAACCAC
PSEN1	NM_000021.3	*WT (L219 site)*	CATTACTGTTGCACTCCTGATC	ATGCCTGCTGGAGTCGAA
PSEN1	NM_000021.3	*L219P mutation*	CATTACTGTTGCACTCCTGATC	GCCTGCTGGAGTCGAGG
PSEN1	NM_000021.3	*WT (G206 site)*	GGTCATCCATGCCTGGC	GGAAATCATTCCCACCACAC
PSEN1	NM_000021.3	*G206V mutation*	GGTCATCCATGCCTGGC	GGAAATCATTCCCACCACAA
PSEN2	NM_012486.2	*WT*	CATGATCGTGGTGGTAGCC	GGATGAACTTGTAGCAGCGG
CYC1	NM_001916	*WT*	AGCCTACAAGAAAGTTTGCCTAT	TCTTCTTCCGGTAGTGGATCTTGGC
RPL13	NM_00977	*WT*	CCTGGAGGAGAAGAGGAAAGAGA	TTGAGGACCTCTGTGTATTTGTCAA
cd44a	XM_001922456	*WT*	CCCATCAGATTCATCACCAAACT	AGAATGAACTGTCTCTGGCTGC
mmp2	NM_198067	*WT*	CCTGAGACAGCAATGTCAACATCA	CATCATTGCGCCCTGATGTG
igfbp3	NM_205751	*WT*	AGTGCAGTCCATCCATCCAAAGGC	GTCTCCATGTTATAGCAGTGGACCT
pdk1	XM_678484	*WT*	ACAACCTGAATATAGTCTTAGC	GTGTGGAGTGTGATGATG

sufficient for one Nu-PAGE gel (i.e. 3 × 10 µl for three lanes). All samples and standards were stored at −80°C until required.

Protein immunoblotting

Samples and standards were prepared by sonication for 10 min followed by incubation at 90°C for 5 min. PrecisionPlusProtein-DualXtra ladder (Bio-Rad, Hercules, California, USA) (7 µl), standards (3 × 10 µl) and samples (6 × ∼18 µl) were loaded on a 4–12% Bis-Tris Nu-PAGE (Life Technologies) gel for electrophoresis. The protein samples and standards were subsequently transferred to a PVDF membrane using the Mini Blot Module transfer system according to the manufacturer's protocol (Thermo Fisher Scientific). To detect the Hif1ab protein, the membrane was initially blocked in 3%w/v skim milk powder followed by incubation in a 1/3000 dilution of the Hif1ab antibody (Gene Tex, Irvine, California, USA, cat no. GTX131826). The membrane was washed and incubated in a 1/2500 dilution of the rabbit-HRP secondary antibody (Sigma-Aldrich). After washing, Hif1ab protein was detected on the membrane using ECL detection reagents (Thermo Fisher Scientific) and visualized using the Chemi Doc Imaging System (Bio-Rad). The Hif1ab protein band can be observed at ∼100 kDa. Using Image Lab software (Bio-Rad), a densitometry analysis was performed for the Hif1ab protein band for each sample and standard. An average value was obtained for the standards for each membrane. Each sample value was then normalized to the average standard value. Each protein sample was quantified using the EZQ protein quantification kit (Thermo Fisher Scientific) according to the manufacturer's protocol. The standard normalized value for each sample was then expressed as Hif1ab per total protein loaded. Each membrane displayed 3 normoxia and 3 hypoxia samples from the same age (6 or 24 months) and the same genotype (+/+, $psen1^{Q96\_K97del}$/+ or $psen1^{K97fs}$/+) together with the protein standard in 3 separate lanes.

L-Lactate content analysis of zebrafish brain

L-Lactate content was analysed using the Lactate Colorimetric Kit II (BioVision Milpitas, California, USA). Brains were removed from zebrafish adults in cold 1× PBS, then weighed and homogenized in the Lactate Assay Buffer provided in the kit. Each sample was then filtered through a 10 kDa MW spin filter (Sartorius Stedim Biotech, Göttingen, Germany) to remove all proteins. The lactate content of the eluate from each zebrafish brain was determined using the kit according to the manufacturer's protocol and the original brain weight was used to calculate the nmol of lactate per mg of brain tissue.

Supplementary Material

Supplementary Material is available at *HMG* online.

Conflict of Interest statement. None declared.

Funding

Australia's National Health and Medical Research Council (1126422); Family of Lindsay Carthew (M.N.); The University of New South Wales; Neuroscience Research Australia; National Institute of Alcohol Abuse and Alcoholism (R24AA012725); National Health and Medical Research Council of Australia (1079679 to G.M.H.); National Health and Medical Research Council of Australia (1037746 and #1095127).

References

1. Mawuenyega, K.G., Sigurdson, W., Ovod, V., Munsell, L., Kasten, T., Morris, J.C., Yarasheski, K.E. and Bateman, R.J. (2010) Decreased clearance of CNS beta-amyloid in Alzheimer's disease. *Science*, **330**, 1774.
2. Villemagne, V.L., Burnham, S., Bourgeat, P., Brown, B., Ellis, K.A., Salvado, O., Szoeke, C., Macaulay, S.L., Martins, R., Maruff, P. *et al.* (2013) Amyloid beta deposition, neurodegeneration, and cognitive decline in sporadic Alzheimer's disease: a prospective cohort study. *Lancet Neurol.*, **12**, 357–367.

3. Bateman, R.J., Xiong, C., Benzinger, T.L., Fagan, A.M., Goate, A., Fox, N.C., Marcus, D.S., Cairns, N.J., Xie, X., Blazey, T.M. *et al.* (2012) Clinical and biomarker changes in dominantly inherited Alzheimer's disease. *N. Engl. J. Med.*, **367**, 795–804.
4. Iturria-Medina, Y., Sotero, R.C., Toussaint, P.J., Mateos-Perez, J.M., Evans, A.C. and Alzheimer's Disease Neuroimaging, I. (2016) Early role of vascular dysregulation on late-onset Alzheimer's disease based on multifactorial data-driven analysis. *Nat. Commun.*, **7**, 11934.
5. Karran, E. and De Strooper, B. (2016) The amyloid cascade hypothesis: are we poised for success or failure? *J. Neurochem.*, **139**, 237–252.
6. Doig, A.J., Del Castillo-Frias, M.P., Berthoumieu, O., Tarus, B., Nasica-Labouze, J., Sterpone, F., Nguyen, P.H., Hooper, N.M., Faller, P. and Derreumaux, P. (2017) Why is research on amyloid-beta failing to give new drugs for Alzheimer's disease? *ACS Chem. Neurosci.*, **8**, 1435–1437.
7. de Bruijn, R.F. and Ikram, M.A. (2014) Cardiovascular risk factors and future risk of Alzheimer's disease. *BMC Med.*, **12**, 130.
8. O'Brien, J.T. and Markus, H.S. (2014) Vascular risk factors and Alzheimer's disease. *BMC Med.*, **12**, 218.
9. Reitz, C. and Mayeux, R. (2014) Alzheimer disease: epidemiology, diagnostic criteria, risk factors and biomarkers. *Biochem. Pharmacol.*, **88**, 640–651.
10. Panza, G.A., Taylor, B.A., MacDonald, H.V., Johnson, B.T., Zaleski, A.L., Livingston, J., Thompson, P.D. and Pescatello, L.S. (2018) Can exercise improve cognitive symptoms of Alzheimer's disease? A meta-analysis. *J. Am. Geriatr. Soc.*, **66**, 487–495.
11. Kirk-Sanchez, N.J. and McGough, E.L. (2014) Physical exercise and cognitive performance in the elderly: current perspectives. *Clin. Interv. Aging*, **9**, 51–62.
12. Daulatzai, M.A. (2017) Cerebral hypoperfusion and glucose hypometabolism: key pathophysiological modulators promote neurodegeneration, cognitive impairment, and Alzheimer's disease. *J. Neurosci. Res.*, **95**, 943–972.
13. Crawford, J.G. (1996) Alzheimer's disease risk factors as related to cerebral blood flow. *Med. Hypotheses*, **46**, 367–377.
14. Moussavi Nik, S.H., Wilson, L., Newman, M., Croft, K., Mori, T.A., Musgrave, I. and Lardelli, M. (2012) The BACE1-PSEN-AbetaPP regulatory axis has an ancient role in response to low oxygen/oxidative stress. *J. Alzheimers Dis.*, **28**, 515–530.
15. Lukiw, W.J., Gordon, W.C., Rogaev, E.I., Thompson, H. and Bazan, N.G. (2001) Presenilin-2 (PS2) expression up-regulation in a model of retinopathy of prematurity and pathoangiogenesis. *Neuroreport*, **12**, 53–57.
16. Tamagno, E., Guglielmotto, M., Aragno, M., Borghi, R., Autelli, R., Giliberto, L., Muraca, G., Danni, O., Zhu, X., Smith, M.A. *et al.* (2008) Oxidative stress activates a positive feedback between the gamma- and beta-secretase cleavages of the beta-amyloid precursor protein. *J. Neurochem.*, **104**, 683–695.
17. Wang, Z., Wu, D. and Vinters, H.V. (2002) Hypoxia and reoxygenation of brain microvascular smooth muscle cells in vitro: cellular responses and expression of cerebral amyloid angiopathy-associated proteins. *APMIS*, **110**, 423–434.
18. Oresic, M., Hyotylainen, T., Herukka, S.K., Sysi-Aho, M., Mattila, I., Seppanan-Laakso, T., Julkunen, V., Gopalacharyulu, P.V., Hallikainen, M., Koikkalainen, J. *et al.* (2011) Metabolome in progression to Alzheimer's disease. *Transl. Psychiatry*, **1**, e57.
19. Liu, Y., Liu, F., Iqbal, K., Grundke-Iqbal, I. and Gong, C.X. (2008) Decreased glucose transporters correlate to abnormal hyperphosphorylation of tau in Alzheimer disease. *FEBS Lett.*, **582**, 359–364.
20. Guerreiro, R. and Hardy, J. (2014) Genetics of Alzheimer's disease. *Neurotherapeutics*, **11**, 732–737.
21. Jayadev, S., Leverenz, J.B., Steinbart, E., Stahl, J., Klunk, W., Yu, C.E. and Bird, T.D. (2010) Alzheimer's disease phenotypes and genotypes associated with mutations in presenilin 2. *Brain*, **133**, 1143–1154.
22. Zhu, X.C., Tan, L., Wang, H.F., Jiang, T., Cao, L., Wang, C., Wang, J., Tan, C.C., Meng, X.F. and Yu, J.T. (2015) Rate of early onset Alzheimer's disease: a systematic review and meta-analysis. *Ann. Transl. Med.*, **3**, 38.
23. Masters, C.L., Bateman, R.J., Blennow, K., Rowe, C.C., Sperling, R.A. and Cummings, J.L. (2015) Alzheimer's disease. *Nat. Rev. Dis. Primers.*, **1**, 1–8.
24. Pottier, C., Hannequin, D., Coutant, S., Rovelet-Lecrux, A., Wallon, D., Rousseau, S., Legallic, S., Paquet, C., Bombois, S., Pariente, J. *et al.* (2012) High frequency of potentially pathogenic SORL1 mutations in autosomal dominant early-onset Alzheimer disease. *Mol. Psychiatry*, **17**, 875–879.
25. Jayne, T., Newman, M., Verdile, G., Sutherland, G., Munch, G., Musgrave, I., Moussavi Nik, S.H. and Lardelli, M. (2016) Evidence for and against a pathogenic role of reduced gamma-secretase activity in familial Alzheimer's disease. *J. Alzheimers Dis.*, **52**, 781–799.
26. Lumsden, A.L., Rogers, J.T., Majd, S., Newman, M., Sutherland, G.T., Verdile, G. and Lardelli, M. (2018) Dysregulation of neuronal iron homeostasis as an alternative unifying effect of mutations causing familial Alzheimer's disease. *Front. Neurosci.*, **12**, 533.
27. Quiroz, Y.T., Schultz, A.P., Chen, K., Protas, H.D., Brickhouse, M., Fleisher, A.S., Langbaum, J.B., Thiyyagura, P., Fagan, A.M., Shah, A.R. *et al.* (2015) Brain imaging and blood biomarker abnormalities in children with autosomal dominant Alzheimer disease: a cross-sectional study. *JAMA Neurol.*, **72**, 912–919.
28. Reiman, E.M., Quiroz, Y.T., Fleisher, A.S., Chen, K., Velez-Pardo, C., Jimenez-Del-Rio, M., Fagan, A.M., Shah, A.R., Alvarez, S., Arbelaez, A. *et al.* (2012) Brain imaging and fluid biomarker analysis in young adults at genetic risk for autosomal dominant Alzheimer's disease in the presenilin 1 E280A kindred: a case-control study. *Lancet Neurol.*, **11**, 1048–1056.
29. Gordon, B.A., Blazey, T.M., Su, Y., Hari-Raj, A., Dincer, A., Flores, S., Christensen, J., McDade, E., Wang, G., Xiong, C. *et al.* (2018) Spatial patterns of neuroimaging biomarker change in individuals from families with autosomal dominant Alzheimer's disease: a longitudinal study. *Lancet Neurol.*, **17**, 241–250.
30. Newman, M., Hin, N., Pederson, S. and Lardelli, M. (2019) Brain transcriptome analysis of a familial Alzheimer's disease-like mutation in the zebrafish presenilin 1 gene implies effects on energy production. *Mol Brain*, **12**, 43. https://doi.org/10.1186/s13041-019-0467-y.
31. Hin, N., Newman, M., Kaslin, J., Douek, A.M., Lumsden, A., Nik, S.H.M., Dong, Y., Zhou, X.F., Manucat-Tan, N.B., Ludington, A. *et al.* (2020) Accelerated brain aging towards transcriptional inversion in a zebrafish model of the K115fs mutation of human PSEN2. *PLoS One*, **15**, e0227258.
32. Braggin, J.E., Bucks, S.A., Course, M.M., Smith, C.L., Sopher, B., Osnis, L., Shuey, K.D., Domoto-Reilly, K., Caso, C., Kinoshita,

C. et al. (2019) Alternative splicing in a presenilin 2 variant associated with Alzheimer disease. *Ann. Clin. Transl. Neurol.*, **6**, 762–777.
33. De Strooper, B. (2007) Loss-of-function presenilin mutations in Alzheimer disease. Talking point on the role of presenilin mutations in Alzheimer disease. *EMBO Rep.*, **8**, 141–146.
34. Wang, B., Yang, W., Wen, W., Sun, J., Su, B., Liu, B., Ma, D., Lv, D., Wen, Y., Qu, T. *et al.* (2010) Gamma-secretase gene mutations in familial acne inversa. *Science*, **330**, 1065.
35. Area-Gomez, E., de Groof, A.J., Boldogh, I., Bird, T.D., Gibson, G.E., Koehler, C.M., Yu, W.H., Duff, K.E., Yaffe, M.P., Pon, L.A. *et al.* (2009) Presenilins are enriched in endoplasmic reticulum membranes associated with mitochondria. *Am. J. Pathol.*, **175**, 1810–1816.
36. Newman, M., Hin, N., Pederson, S. and Lardelli, M. (2019) Brain transcriptome analysis of a familial Alzheimer's disease-like mutation in the zebrafish presenilin 1 gene implies effects on energy production. *Mol. Brain*, **12**, 43.
37. De Gasperi, R., Sosa, M.A., Dracheva, S. and Elder, G.A. (2010) Presenilin-1 regulates induction of hypoxia inducible factor-1alpha: altered activation by a mutation associated with familial Alzheimer's disease. *Mol. Neurodegener.*, **5**, 38.
38. Villa, J.C., Chiu, D., Brandes, A.H., Escorcia, F.E., Villa, C.H., Maguire, W.F., Hu, C.J., de Stanchina, E., Simon, M.C., Sisodia, S.S. *et al.* (2014) Nontranscriptional role of Hif-1alpha in activation of gamma-secretase and notch signaling in breast cancer. *Cell Rep.*, **8**, 1077–1092.
39. Harris, A.L. (2002) Hypoxia–a key regulatory factor in tumour growth. *Nat. Rev. Cancer*, **2**, 38–47.
40. Kim, J.W., Tchernyshyov, I., Semenza, G.L. and Dang, C.V. (2006) HIF-1-mediated expression of pyruvate dehydrogenase kinase: a metabolic switch required for cellular adaptation to hypoxia. *Cell Metab.*, **3**, 177–185.
41. Paolicchi, E., Gemignani, F., Krstic-Demonacos, M., Dedhar, S., Mutti, L. and Landi, S. (2016) Targeting hypoxic response for cancer therapy. *Oncotarget*, **7**, 13464–13478.
42. Kuang, X., Liu, C., Fang, J., Ma, W., Zhang, J. and Cui, S. (2016) The tumor suppressor gene lkb1 is essential for glucose homeostasis during zebrafish early development. *FEBS Lett.*, **590**, 2076–2085.
43. Caceda, R., Gamboa, J.L., Boero, J.A., Monge, C.C. and Arregui, A. (2001) Energetic metabolism in mouse cerebral cortex during chronic hypoxia. *Neurosci. Lett.*, **301**, 171–174.
44. Gerhard, G.S., Kauffman, E.J., Wang, X., Stewart, R., Moore, J.L., Kasales, C.J., Demidenko, E. and Cheng, K.C. (2002) Life spans and senescent phenotypes in two strains of Zebrafish (Danio rerio). *Exp. Gerontol.*, **37**, 1055–1068.
45. He, F. and Jacobson, A. (2015) Nonsense-mediated mRNA decay: degradation of defective transcripts is only part of the story. *Annu. Rev. Genet.*, **49**, 339–366.
46. El-Brolosy, M.A., Kontarakis, Z., Rossi, A., Kuenne, C., Gunther, S., Fukuda, N., Kikhi, K., Boezio, G.L.M., Takacs, C.M., Lai, S.L. *et al.* (2019) Genetic compensation triggered by mutant mRNA degradation. *Nature*, **568**, 193–197.
47. Ndubuizu, O.I., Chavez, J.C. and LaManna, J.C. (2009) Increased prolyl 4-hydroxylase expression and differential regulation of hypoxia-inducible factors in the aged rat brain. *Am. J. Physiol. Regul. Integr. Comp. Physiol.*, **297**, R158–R165.
48. Ndubuizu, O.I., Tsipis, C.P., Li, A. and LaManna, J.C. (2010) Hypoxia-inducible factor-1 (HIF-1)-independent microvascular angiogenesis in the aged rat brain. *Brain Res.*, **1366**, 101–109.
49. Blair, J.E. and Hedges, S.B. (2005) Molecular phylogeny and divergence times of deuterostome animals. *Mol. Biol. Evol.*, **22**, 2275–2284.
50. Lu, T., Pan, Y., Kao, S.Y., Li, C., Kohane, I., Chan, J. and Yankner, B.A. (2004) Gene regulation and DNA damage in the ageing human brain. *Nature*, **429**, 883–891.
51. Patel, A., Malinovska, L., Saha, S., Wang, J., Alberti, S., Krishnan, Y. and Hyman, A.A. (2017) ATP as a biological hydrotrope. *Science*, **356**, 753–756.
52. Kaufmann, T., van der Meer, D., Doan, N.T., Schwarz, E., Lund, M.J., Agartz, I., Alnaes, D., Barch, D.M., Baur-Streubel, R., Bertolino, A. *et al.* (2019) Common brain disorders are associated with heritable patterns of apparent aging of the brain. *Nat. Neurosci.*, **22**, 1617–1623.
53. Eberling, J.L., Jagust, W.J., Reed, B.R. and Baker, M.G. (1992) Reduced temporal lobe blood flow in Alzheimer's disease. *Neurobiol. Aging*, **13**, 483–491.
54. Johnson, K.A., Jones, K., Holman, B.L., Becker, J.A., Spiers, P.A., Satlin, A. and Albert, M.S. (1998) Preclinical prediction of Alzheimer's disease using SPECT. *Neurology*, **50**, 1563–1571.
55. Raz, L., Bhaskar, K., Weaver, J., Marini, S., Zhang, Q., Thompson, J.F., Espinoza, C., Iqbal, S., Maphis, N.M., Weston, L. *et al.* (2019) Hypoxia promotes tau hyperphosphorylation with associated neuropathology in vascular dysfunction. *Neurobiol. Dis.*, **126**, 124–136.
56. Mesulam, M.M. (1999) Neuroplasticity failure in Alzheimer's disease: bridging the gap between plaques and tangles. *Neuron*, **24**, 521–529.
57. Berchtold, N.C., Sabbagh, M.N., Beach, T.G., Kim, R.C., Cribbs, D.H. and Cotman, C.W. (2014) Brain gene expression patterns differentiate mild cognitive impairment from normal aged and Alzheimer's disease. *Neurobiol. Aging*, **35**, 1961–1972.
58. Head, E., Lott, I.T., Patterson, D., Doran, E. and Haier, R.J. (2007) Possible compensatory events in adult down syndrome brain prior to the development of Alzheimer disease neuropathology: targets for nonpharmacological intervention. *J. Alzheimers Dis.*, **11**, 61–76.
59. Arnemann, K.L., Stober, F., Narayan, S., Rabinovici, G.D. and Jagust, W.J. (2018) Metabolic brain networks in aging and preclinical Alzheimer's disease. *Neuroimage Clin.*, **17**, 987–999.
60. Moussavi Nik, S.H., Newman, M., Wilson, L., Ebrahimie, E., Wells, S., Musgrave, I., Verdile, G., Martins, R.N. and Lardelli, M. (2015) Alzheimer's disease-related peptide PS2V plays ancient, conserved roles in suppression of the unfolded protein response under hypoxia and stimulation of gamma-secretase activity. *Hum. Mol. Genet.*, **24**, 3662–378.
61. Sato, N., Hori, O., Yamaguchi, A., Lambert, J.C., Chartier-Harlin, M.C., Robinson, P.A., Delacourte, A., Schmidt, A.M., Furuyama, T., Imaizumi, K. *et al.* (1999) A novel presenilin-2 splice variant in human Alzheimer's disease brain tissue. *J. Neurochem.*, **72**, 2498–2505.
62. Katayama, T., Imaizumi, K., Manabe, T., Hitomi, J., Kudo, T. and Tohyama, M. (2004) Induction of neuronal death by ER stress in Alzheimer's disease. *J. Chem. Neuroanat.*, **28**, 67–78.
63. Heilig, E.A., Gutti, U., Tai, T., Shen, J. and Kelleher, R.J., 3rd. (2013) Trans-dominant negative effects of pathogenic PSEN1

mutations on gamma-secretase activity and Abeta production. *J. Neurosci.*, **33**, 11606–11617.
64. Pera, M., Larrea, D., Guardia-Laguarta, C., Montesinos, J., Velasco, K.R., Agrawal, R.R., Xu, Y., Chan, R.B., Di Paolo, G., Mehler, M.F. *et al.* (2017) Increased localization of APP-C99 in mitochondria-associated ER membranes causes mitochondrial dysfunction in Alzheimer disease. *EMBO J.*, **36**, 3356–3371.
65. Takami, K., Terai, K., Matsuo, A., Walker, D.G. and McGeer, P.L. (1997) Expression of presenilin-1 and -2 mRNAs in rat and Alzheimer's disease brains. *Brain Res.*, **748**, 122–130.
66. Isoe-Wada, K., Urakami, K., Wakutani, Y., Adachi, Y., Arai, H., Sasaki, H. and Nakashima, K. (1999) Alteration in brain presenilin-1 mRNA expression in sporadic Alzheimer's disease. *Eur. J. Neurol.*, **6**, 163–167.
67. Ikeda, K., Urakami, K., Arai, H., Wada, K., Wakutani, Y., Ji, Y., Adachi, Y., Okada, A., Kowa, H., Sasaki, H. *et al.* (2000) The expression of presenilin 1 mRNA in skin fibroblasts and brains from sporadic Alzheimer's disease. *Dement. Geriatr. Cogn. Disord.*, **11**, 245–250.
68. Borghi, R., Piccini, A., Barini, E., Cirmena, G., Guglielmotto, M., Tamagno, E., Fornaro, M., Perry, G., Smith, M.A., Garuti, A. *et al.* (2010) Upregulation of presenilin 1 in brains of sporadic, late-onset Alzheimer's disease. *J. Alzheimers Dis.*, **22**, 771–775.
69. Farnsworth, B., Peuckert, C., Zimmermann, B., Jazin, E., Kettunen, P. and Emilsson, L.S. (2016) Gene expression of quaking in sporadic Alzheimer's disease patients is both upregulated and related to expression levels of genes involved in amyloid plaque and neurofibrillary tangle formation. *J. Alzheimers Dis.*, **53**, 209–219.
70. Johnston, J.A., Froelich, S., Lannfelt, L. and Cowburn, R.F. (1996) Quantification of presenilin-1 mRNA in Alzheimer's disease brains. *FEBS Lett.*, **394**, 279–284.
71. Delabio, R., Rasmussen, L., Mizumoto, I., Viani, G.A., Chen, E., Villares, J., Costa, I.B., Turecki, G., Linde, S.A., Smith, M.C. *et al.* (2014) PSEN1 and PSEN2 gene expression in Alzheimer's disease brain: a new approach. *J. Alzheimers Dis.*, **42**, 757–760.
72. Qiu, C. and Fratiglioni, L. (2018) Aging without dementia is achievable: current evidence from epidemiological research. *J. Alzheimers Dis.*, **62**, 933–942.
73. Boeve, B., McCormick, J., Smith, G., Ferman, T., Rummans, T., Carpenter, T., Ivnik, R., Kokmen, E., Tangalos, E., Edland, S. *et al.* (2003) Mild cognitive impairment in the oldest old. *Neurology*, **60**, 477–480.
74. Andersen-Ranberg, K., Vasegaard, L. and Jeune, B. (2001) Dementia is not inevitable: a population-based study of Danish centenarians. *J. Gerontol. B Psychol. Sci. Soc. Sci.*, **56**, P152–P159.
75. Hin, N., Newman, M., Pederson, S. and Lardelli, M. (2020) Iron responsive element (IRE)-mediated responses to iron dyshomeostasis in Alzheimer's disease. *bioRxiv*, in press, 2020.2005.2001.071498.
76. Skaggs, K., Goldman, D. and Parent, J.M. (2014) Excitotoxic brain injury in adult zebrafish stimulates neurogenesis and long-distance neuronal integration. *Glia*, **62**, 2061–2079.
77. Solchenberger, B., Russell, C., Kremmer, E., Haass, C. and Schmid, B. (2015) Granulin knock out zebrafish lack frontotemporal lobar degeneration and neuronal ceroid lipofuscinosis pathology. *PLoS One*, **10**, e0118956.
78. Le Moan, N., Houslay, D.M., Christian, F., Houslay, M.D. and Akassoglou, K. (2011) Oxygen-dependent cleavage of the p75 neurotrophin receptor triggers stabilization of HIF-1alpha. *Mol. Cell*, **44**, 476–490.
79. Peyssonnaux, C., Zinkernagel, A.S., Schuepbach, R.A., Rankin, E., Vaulont, S., Haase, V.H., Nizet, V. and Johnson, R.S. (2007) Regulation of iron homeostasis by the hypoxia-inducible transcription factors (HIFs). *J. Clin. Invest.*, **117**, 1926–1932.
80. Lane, D.J., Merlot, A.M., Huang, M.L., Bae, D.H., Jansson, P.J., Sahni, S., Kalinowski, D.S. and Richardson, D.R. (2015) Cellular iron uptake, trafficking and metabolism: key molecules and mechanisms and their roles in disease. *Biochim. Biophys. Acta*, **1853**, 1130–1144.
81. Yambire, K.F., Rostosky, C., Watanabe, T., Pacheu-Grau, D., Torres-Odio, S., Sanchez-Guerrero, A., Senderovich, O., Meyron-Holtz, E.G., Milosevic, I., Frahm, J. *et al.* (2019) Impaired lysosomal acidification triggers iron deficiency and inflammation in vivo. *Elife*, **8**, e51031. doi: 10.7554/eLife.51031.
82. Muller, S., Preische, O., Sohrabi, H.R., Graber, S., Jucker, M., Ringman, J.M., Martins, R.N., McDade, E., Schofield, P.R., Ghetti, B. *et al.* (2018) Relationship between physical activity, cognition, and Alzheimer pathology in autosomal dominant Alzheimer's disease. *Alzheimers Dement.*, **14**, 1427–1437.
83. Santos-Lozano, A., Pareja-Galeano, H., Sanchis-Gomar, F., Quindos-Rubial, M., Fiuza-Luces, C., Cristi-Montero, C., Emanuele, E., Garatachea, N. and Lucia, A. (2016) Physical activity and Alzheimer disease: a protective association. *Mayo Clin. Proc.*, **91**, 999–1020.
84. Stephen, R., Hongisto, K., Solomon, A. and Lonnroos, E. (2017) Physical activity and Alzheimer's disease: a systematic review. *J. Gerontol. A Biol. Sci. Med. Sci.*, **72**, 733–739.
85. Beydoun, M.A., Beydoun, H.A., Gamaldo, A.A., Teel, A., Zonderman, A.B. and Wang, Y. (2014) Epidemiologic studies of modifiable factors associated with cognition and dementia: systematic review and meta-analysis. *BMC Public Health*, **14**, 643.
86. Frederiksen, K.S., Gjerum, L., Waldemar, G. and Hasselbalch, S.G. (2018) Effects of physical exercise on Alzheimer's disease biomarkers: a systematic review of intervention studies. *J. Alzheimers Dis.*, **61**, 359–372.
87. Fazekas de St, G. (1982) The evaluation of limiting dilution assays. *J. Immunol. Methods*, **49**, R11–R23.